

RESEARCH

Open Access



Corrosion of carbon steel rebar in binary blended concrete with accelerated chloride transport

Kazi Naimul Hoque¹, Francisco Presuel-Moreno^{1*} and Manzurul Nazim¹

Abstract

Samples with two different binary blended concrete mixes were prepared, one containing cement replacement of 50% slag (referred here as SL mix) and the other containing cement replacement of 20% fly ash (termed here as FA mix). The water to cementitious ratio used to produce concrete specimens was 0.41. On the top surface of each specimen, various reservoir lengths that ranged from 2.5 cm to 17.5 cm were fitted, and these reservoirs were filled with a 10% NaCl solution. Electromigration was used to accelerate the transport of chlorides, with an applied potential of 9 V at first, and subsequently reduced to 3 V after about a week. The electromigration was applied for a short period (few weeks to a couple of months). For a period of about 1100 days, the corrosion related parameters such as concrete solution resistance, rebar potential, and corrosion current were monitored via the rebar potential measurements, linear polarization resistance (LPR) and electrochemical impedance spectroscopy (EIS) measurements, the latter used only to obtain the solution resistance. The corrosion current values determined through experimental observations were then converted to mass loss using Faraday's law. The readings of corrosion current values (last 7 sets of readings) as well as the calculated mass loss values were found to be larger for the rebars embedded in specimens prepared with SL mix, followed by rebars embedded in specimens prepared with FA mix. Corrosion current and calculated mass loss values in general tended to increase with increasing solution reservoir lengths. No cracks or corrosion products that reached the surface of the concrete were observed on the specimens for the duration of the reported monitored propagation period. This study offers a framework for future studies on accelerated steel corrosion in concrete.

Keywords Accelerated chloride transport, Reservoir length, Fly ash, Slag, Corrosion current, Mass loss

*Correspondence:

Francisco Presuel-Moreno
fpresuel@fau.edu

¹Department of Ocean and Mechanical Engineering, Florida Atlantic University (FAU), Dania Beach, Florida 33004, USA

Introduction

Corrosion of steel reinforcement is one of the primary mechanisms that causes reinforced concrete (RC) constructions to degrade in temperate, marine, and high humidity conditions. If the issue isn't resolved, it accelerates the deterioration of RC structures and may have several interconnected negative effects, including a reduction in the RC structure's service life and loss of steel cross-section area. Although corrosion of steel in RC structures are primarily caused by the ingress of carbon dioxide (carbonation-induced corrosion) or chlorides (chloride-induced corrosion), the latter is the predominant cause. The natural rate of chloride penetration is often slow, whether steel corrosion is driven by carbonation or chloride, making it difficult to obtain information that may be utilized to make decisions with short term experiments. The problem is worsened due to the scarcity of research and limited findings concerning the initiation and propagation of natural corrosion. [1–5]. These investigations demonstrate that significant corrosion-induced damage in RC structures undergoing natural corrosion requires longer monitoring durations.

Steel corrosion that occurs in concrete at a rate that is faster than the corresponding natural process is known as “accelerated corrosion of steel.” Unlike natural corrosion, the effects of accelerated corrosion, such as depassivation and/or corrosion-induced damage, can be seen rather quickly. Anodic and cathodic reactions take place in both environments, which is one similarity between natural and accelerated corrosion [6]. In the past, accelerated corrosion techniques have been utilized to investigate the commencement of corrosion, corrosion-induced damage, and the effects on variables such as deformation behavior, ductility, bond strength, and failure mechanisms in RC structures [7–10]. However, due to the current requirement to quantify and account for the corrosion propagation phase in the serviceability of corrosion-affected RC structures [11–13], it is necessary to research and develop techniques that, while simulating the natural corrosion propagation, can eliminate the initiation phase without significantly increasing corrosion-induced damage, if any.

Chloride-induced corrosion can be accelerated using a variety of methods, including admixed chlorides, cyclic wetting and drying with a chloride-solution, applying an anodic impressed current (galvanostatically) or (potentiostatically) between the steel reinforcement (anode) and a separate (internal or external) cathode (e.g., stainless steel), or a suitable combination of these. The steel is artificially polarized by the application of an impressed current (IC) [14]. The penetration of chloride ions (Cl^-) in concrete when impressed current or electric field is applied, is migration-dominated as opposed to natural chloride ingress into concrete through diffusion. When

anodic IC is applied, the entire exposed surface area of the steel becomes anodic, causing widespread corrosion as opposed to the pitting-type corrosion that naturally happens with discrete anodes and cathodes (high cathode-to-anode area ratio). In addition, the anodic IC applied around the steel alters the local chemistry of the concrete pore solution by changing its ionic distribution. Because it offers the advantage of being able to monitor the degree of corrosion, this method is suggested when investigating the degree of steel corrosion in concrete and its impact on variables like flexural strength and ductility. One of the important factors that determines the useful service life of corroding RC structures is the extent of corrosion [7].

Admixed chlorides, which typically range between 1 and 5% by mass of cement, are mainly used in accelerated corrosion investigations to minimize the corrosion initiation phase [7, 15, 16]. The procedure prevents the steel from developing a passive protective coating prior to the chloride threshold being achieved. It also eliminates the chloride binding effects that may occur naturally and is quite likely to alter the alkalinity of the concrete pore solution. By permitting chlorides to quickly penetrate the concrete through capillary suction in addition to diffusion [8–10], cyclic wetting and drying technique expedites steel corrosion in concrete. This is done by allowing dissolved oxygen to be replenished at the steel surface during the drying cycle to support the cathodic reaction mechanism.

For this study, two different binary blended concrete mixtures were prepared. Electromigration accelerated the transport of chloride. The method was developed using the findings of previous research [17]. With this method, the embedded rebar typically starts to corrode after a few weeks or months. The corrosion propagation stage was observed using measurements of electrochemical impedance spectroscopy (EIS) and linear polarization resistance (LPR). The solution resistance, rebar potential, and corrosion current measurements were monitored for about 1100 days.

Experimental details

Concrete mixes, casting and curing of specimens

Concrete specimens of dimensions 30.5 cm x 12.7 cm x 7.6 cm (12 in x 5 in x 3 in) were prepared with a w/cm ratio of 0.41. Two different binder types (80/20 PC/FA, 50/50 PC/SL) were prepared, where PC stands for Portland cement, FA for fly ash, and SL for slag. Table 1 summarizes the mix proportions. Details of each concrete mixes are provided in Appendix 2 [18]. Each specimen contained a carbon steel reinforcing bar with a diameter of 0.94 cm, embedded at a concrete cover of 0.75 cm (0.3 in). Eleven single rebar specimens per mix (for both SL

Table 1 Concrete mix detail for SL and FA specimens

Mix	Cast Date	Cementitious Content	Cement Content	20% FA	8% SF	50% Slag	Fine agg.	Coarse agg.	w/cm ratio
		(kg/m ³)							
SL	4/4/2016	390	195	0	0	195	782	1009	0.41
FA	4/18/2016	390	312	78	0	0	967	833	0.41

and FA concrete mixes), a total of 22 specimens were prepared.

Rebar segments were cut to size. The rebars were wire brushed. Hexane was used to eliminate any grease from the reinforcement before casting. Prior to casting the concrete, each rebar had a machine stainless-steel screw installed after it had been drilled and tapped on one end. This method established an electrical contact for the purpose of monitoring corrosion. The mold side became the sample top surface during exposure. At the time of casting, stainless steel (or titanium mix metal oxide, or “TiMMO”) mesh was placed on the top side of each specimen. Throughout the experiment, this surface served as the bottom surface. The mesh accelerated the transfer of chlorides. Meshes ranged in length from 2.5 to 17.5 cm, were positioned in the center of the rebar, and were roughly 3 cm wide. The specimens were prepared at the State Materials Office (SMO) of the Florida Department of Transportation (FDOT). After one day, the molds were taken out and stored in the fog chamber to cure for at least 28 days.

Specimen setup preparation for electromigration

After casting, the samples were moved to the Marine Materials & Corrosion Laboratory at the FAU SeaTech campus for the experiment’s next phase. These samples were stored there until the solution reservoir was set up in a high humidity chamber. The samples were then placed in laboratory RH environment (65% RH and 21 °C) for a couple of days before installing the solution reservoir. When the solution reservoirs were installed for ponding, the samples were left in the laboratory environment (during electromigration and propagation periods).

A plastic reservoir was attached to the top surface using marine adhesives (which served as the mold surface during casting). At least forty days after casting, the reservoir was installed. The reservoir was filled with NaCl solution (10% NaCl by weight). Several corroding lengths were intended. Toward this goal, the reservoir length limited the area where corrosion could commence. After installing the reservoirs, the samples were stored in high humidity for 3 to 7 days. On the top surface of the solution reservoir, electrodes (made of stainless steel wire mesh or TiMMO mesh) with dimensions comparable to those embedded were positioned.

The samples were stored in clear plastic containers. Around one centimeter of the concrete specimen was immersed in a saturated calcium hydroxide solution for each specimen. A white plastic mesh was placed on top of each sample (acrylic perforated). This process was utilized to minimize concrete leaching during the electromigration process.

Electromigration

A potential hold between the top and bottom mesh was established using a power supply. An electric field then forces the chlorides in the solution reservoir into the concrete and in the direction of the embedded rebar. The electrode in the NaCl solution was attached to the power supply’s negative terminal. Each specimen’s embedded mesh had a connection to the positive terminal of the power supply. An acrylic mesh was introduced into the solution reservoir to reduce direct contact between the titanium mix metal oxide wire mesh and the concrete surface. Figure 1 depicts the electromigration experimentation setup.

The labels for each sample are displayed in Tables 2 and 3. The sample name/ID, reservoir length, and the starting and ending dates of electromigration are also included in each of these tables. There is also a column in Tables 2 and 3 that highlights the calculated Ampere-hour applied (integrated values). Each specimen went through several electromigration periods between the start and the end dates listed, but there were several days/weeks with the system off.

Electromigration was carried out on each specimen. The applied potential was 9 V initially. When the electric field was on, the rebar potential was measured with respect to a saturated calomel reference electrode, and a potential larger than +2 V was observed. The applied potential was reduced to 3 V after seven days. Using the delta potential across a 100-ohm resistor, the amount of current applied when a specific voltage was supplied for multiple days at a time was determined. The potential of the rebar was evaluated when the system was turned off. The applied electric field produced an ionic current that polarized the rebars even though they weren’t connected during the electromigration process. After monitoring the rebar potential for some time (usually up to two hours) with the system disconnected, the applied potential was restarted if the most recent measurement of the

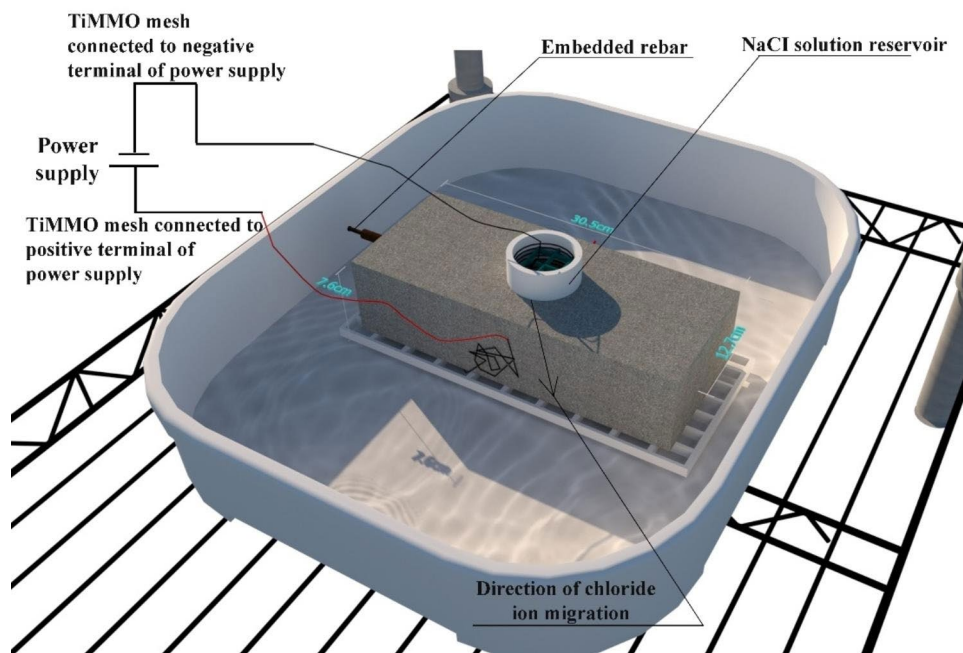


Fig. 1 Experimental setup used for electromigration

Table 2 Single rebar samples made with slag replacement

Sample Number	Reservoir Length (cm)	Migration Time Started	Migration Ending Date	Total Am- pere Hour	Duration days
SL-1	17.5	07/29/16	09/05/16	1.701	27
SL-2	17.5	07/29/16	01/04/17	1.47	50
SL-3	17.5	07/26/16	08/15/16	3.162	16
SL-4	2.5	07/26/16	01/10/17	3.66	54
SL-5	2.5	07/26/16	01/04/17	3.701	82
SL-6	5	07/26/16	01/04/17	4.016	84
SL-7	5	07/26/16	01/04/17	2.482	64
SL-8	5	07/26/16	01/04/17	2.351	84
SL-9	10	07/26/16	01/04/17	4.282	82
SL-10	10	07/26/16	01/04/17	2.369	55
SL-11	10	07/26/16	12/09/16	3.438	49

Table 3 Single rebar samples made with fly ash replacement

Sample Number	Res- ervoir Length (cm)	Migra- tion Time Started	Migra- tion Ending Date	Total Am- pere Hour	Duration days
FA-1	5	07/26/16	01/04/17	4.069	84
FA-2	5	07/26/16	01/04/17	3.015	74
FA-3	5	07/26/16	08/15/16	1.718	16
FA-4	7.5	07/26/16	08/15/16	5.889	16
FA-5	7.5	07/26/16	08/15/16	3.524	25
FA-6	7.5	07/26/16	09/05/16	3.729	30
FA-7	17.5	07/26/16	11/28/16	8.145	64
FA-8	17.5	07/26/16	01/04/17	6.942	74
FA-9	17.5	07/26/16	12/09/16	6.676	65
FA-10	2.5	07/26/16	12/09/16	2.742	64
FA-11	2.5	07/26/16	12/09/16	3.531	73

rebar potential revealed that corrosion had not commenced. On several occasions the time off lasted several days. The process of electromigration was continued until the sample showed an off-rebar potential (a value of $-0.200 V_{sce}$ or more negative), which may indicate the beginning of corrosion in that embedded rebar. According to prior investigations [17], corrosion was reported to have initiated at a potential value of $-0.150 V_{sce}$ ($\sim -0.220 V$ vs. copper sulfate electrode/CSE). A few samples were subjected to very modest anodic polarization (less than $5 \mu A$) for short periods of time (ranged from few days to a few weeks).

Electrochemical measurements for monitoring corrosion

In the occasions when the electromigration system was off for an extended period of time (at least two days), the concrete solution resistance (R_s) and corrected polarization resistance (R_c) were measured. The apparent polarization resistance minus the solution resistance provides the R_c value. The frequency range for the EIS test was 10 kHz to 1 Hz, and the impedance magnitude used for the solution resistance (R_s) was the value measured at a frequency of 54.51 Hz. Initially, the LPR test ranged from 10 mV below the open circuit potential to 1 mV above it. The LPR test was carried out from the open circuit potential to 8 mV below it after around six months of monitoring. The scan rate was chosen to be either 0.1 mV/s or 0.05 mV/s.

The rebar potential, EIS, and LPR measurements described above were carried out during the electromigration period (but after the system had been off for at least two days). In general, these types of measurements were carried out once every month during the corrosion propagation stage (no electromigration took place after day 85). Rc values obtained from LPR readings were converted to corrosion current (I_{corr}), where the corroding area is unknown. The I_{corr} values were then converted to mass loss using Faradaic law calculation. The I_{corr} was determined using the Stern-Geary equation i.e., $I_{corr} = B/R_p$ where R_p is the polarization resistance (defined previously as Rc) and B is the Stern-Geary coefficient that ranged from 13 to 52 mV depending on the steel's corrosion condition (i.e., passive, or active). Most of the research [19, 20] have determined and used values of 26 mV for corroding (active) steel in concrete and 52 mV for passive steel. Therefore, a value of 26 mV was chosen for this study.

Results and discussion

Evolution of rebar potential, Rs, and Rc for SL & FA samples

In the figures in this section and next section, day zero does not correspond to the age of the specimen but rather to the day when solution was poured into the reservoirs. The dashed lines are followed (to the right of them) by an arrow mark, which designates the after-migration period. If there are two black dashed lines, the range represents the overall amount of time that the samples were subjected to electromigration process, and the blue prisms inside represent the approximate amount of time that the electric field was applied. As some of the samples went through slightly accelerated corrosion mechanism by means of a modest applied current, a blue solid line was used to indicate the beginning of this process and the gray columns indicate each instance where applied current took place. For ease of comparison specimens with similar reservoir lengths are compared together. Figure 2 shows the comparison in rebar potential, Rs and Rc value trend for various samples according to their reservoir size respectively.

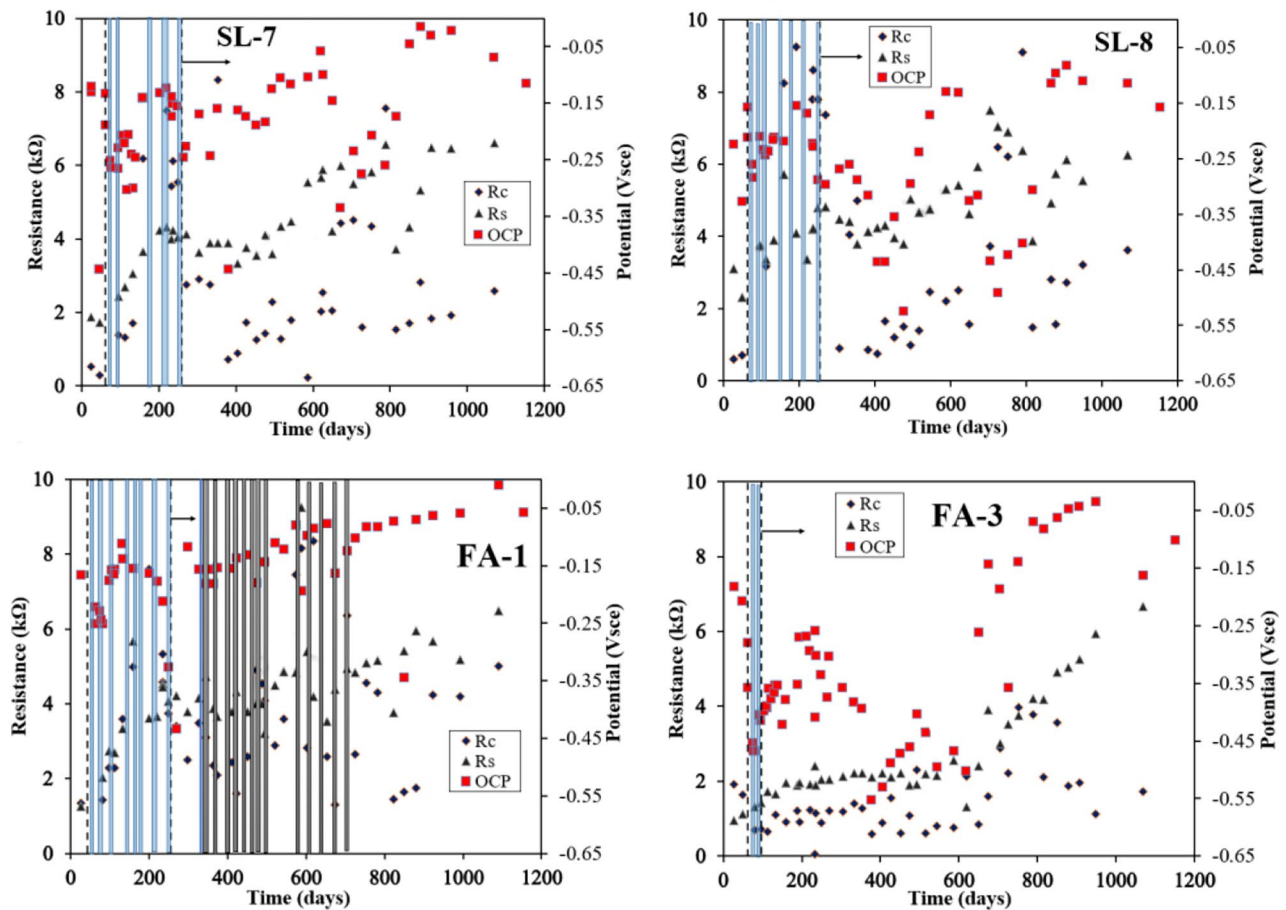


Fig. 2 Rs, Rc, and rebar potential measured on selected rebars under 5 cm reservoir

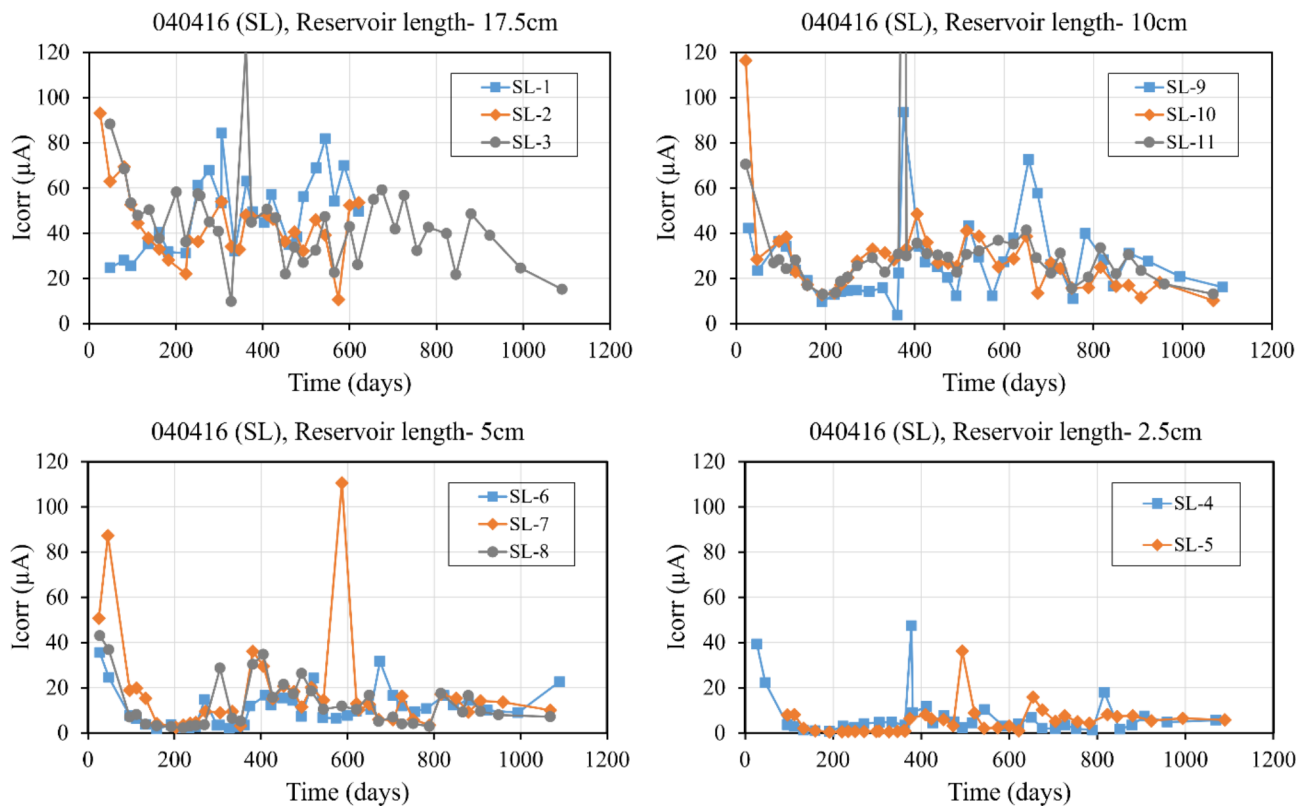


Fig. 3 Icorr (corrosion current) with time obtained from LPR method on selected rebars for SL samples under different size reservoirs

Figure 2 shows four plots describing the rebar potential, R_s and R_c evolution for four different samples with rebars under 5 cm solution reservoir. The SL-7, SL-8, FA-1, and FA-3 all had a reservoir size of 5 cm. It is interesting to note the variety of potential ranges observed. The rebar potential values for the rebar in SL-7 dropped significantly after removing electromigration, reaching a value of around -0.435 Vsce at day 390, tended to drift towards more positive values thereafter. R_c values for the rebar in SL-7 were mostly kept below 3 k Ω throughout the monitored period. Regarding rebar embedded in sample SL-8, after removing electromigration, there was a substantial decrease in both the rebar potential and R_c values. The rebar potential values began to shift towards more positive values from day 490 onwards, while the R_c values exhibited an oscillating pattern subsequently. Although the rebar in FA-1 exhibited a more negative trend for its rebar potential during the initial stages of electromigration, the rebar potential reached -0.155 Vsce after electromigration was eliminated on day 295, with a R_c value that exceed 2 k Ω . Subsequently, the rebar potential showed a monotonic increase from day 340 onwards to the entire monitoring period thereafter, while the R_c values tended to exhibit an oscillating pattern. The sample FA-1 was subjected to modest anodic polarization around day 330, which persisted until approximately day 690. The rebar in FA-3 required a comparatively shorter

period of electromigration when compared to other samples with similar reservoir sizes. The rebar potential values for the FA-3 sample were recorded at -0.468 Vsce on day 81, then showed a monotonic increase until day 220, followed by potential value dropped to -0.502 Vsce on day 619, and tended to shift towards more positive values thereafter. Throughout the monitoring period, the R_c values for the rebar in FA-3 remained mostly below 2 k Ω . For all these samples, the rebar potential values demonstrated a tendency to drift towards more positive values as the days progressed. The rebar potential values measured at day 1069 were -0.070 Vsce (SL-7), -0.114 Vsce (SL-8), -0.011 Vsce (FA-1), and -0.163 Vsce (FA-3). Reference [21] presents the plots for the other SL and FA specimens.

Evolution of corrosion current

The following section shows how corrosion current (I_{corr}) changed over time as determined by LPR measurements for various samples. For SL and FA samples, the I_{corr} plots correspond to the values measured for around 1100 days using the LPR method.

The evolution of corrosion current (I_{corr}) with time obtained from LPR method for SL single rebar samples under different size solution reservoirs are shown in Fig. 3. In the case of samples with 17.5 cm solution reservoir length, it is observed that all the samples (SL-1, SL-2,

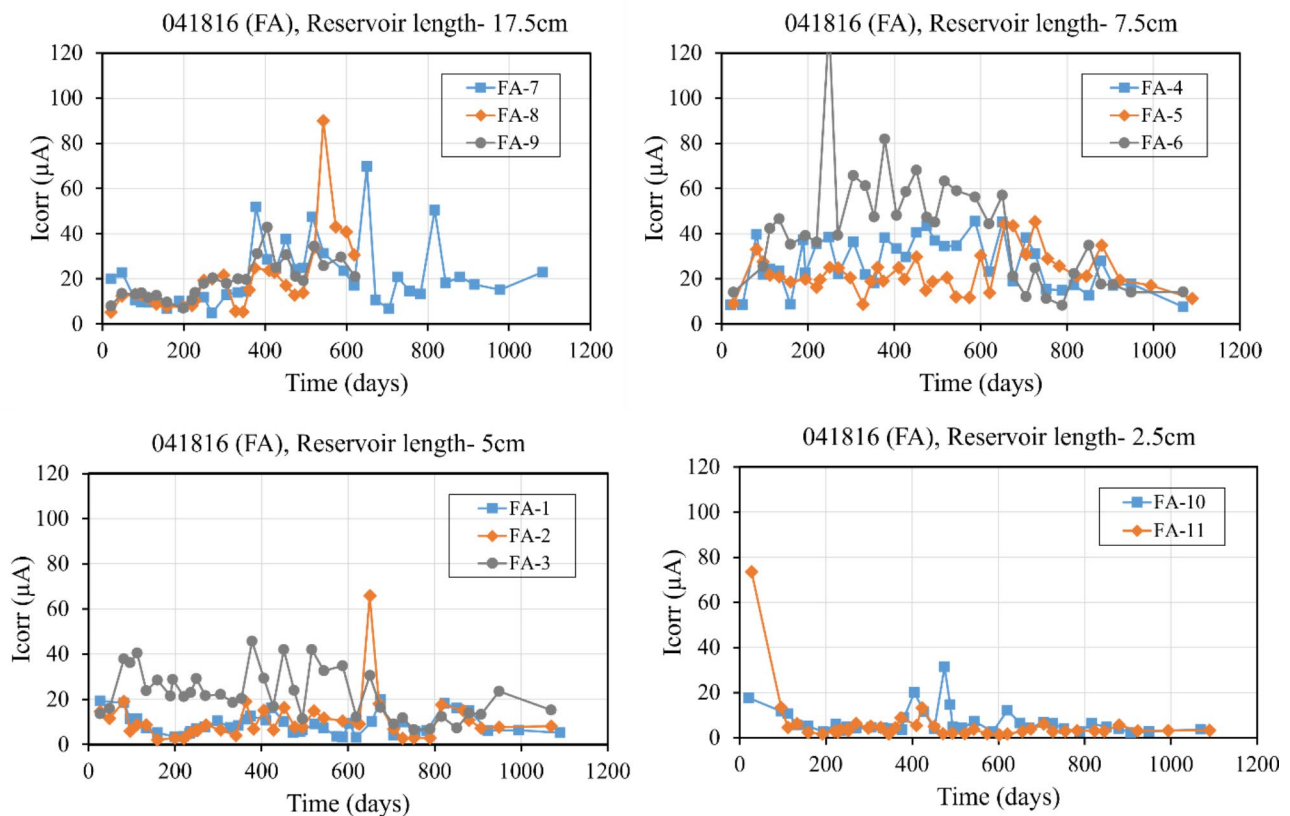


Fig. 4 I_{corr} (corrosion current) with time obtained from LPR method on selected rebars for FA samples under different size reservoirs

and SL-3) showed oscillating trend in terms of corrosion current with time. Samples SL-1 and SL-2 were terminated at around day 620. I_{corr} values ranged from 24.6 to 84.2 μA for SL-1 sample, 16.0–43.7 μA for SL-2 sample, and 20.5–44.5 μA for SL-3 sample. It is to be noted that SL-1 and SL-2 samples were terminated after approximately 600 days. When looking at the I_{corr} plots for samples with 10 cm solution reservoir length, it is noted that SL-9, SL-10, and SL-11 samples showed oscillating trend with time as well. I_{corr} values ranged from 3.8 to 93.5 μA for SL-9 sample, 10.2–116.4 μA for SL-10 sample, and 13.3–70.5 μA for SL-11 sample. Most I_{corr} values were less than 40 μA . In the case of 5 cm solution reservoir length, it is found that SL-6 sample showed a decreasing trend initially, followed by an oscillating trend throughout the monitored period and I_{corr} values ranged from 1.8 to 35.6 μA . A significant decrease of corrosion current was observed for SL-7 sample until day 180, therefore represented an oscillating pattern with time, having only one excursion to a value of 110.6 μA at day 585, with most other values being less than 20 μA . For SL-8 sample, the corrosion current values were mostly less than 20 μA throughout the monitored period and ranged from 2.3 to 43.0 μA in terms of I_{corr} values. While observing I_{corr} plots for 2.5 cm solution reservoir length, it is observed that for SL-4 sample, I_{corr} value dropped significantly

around day 160, showed slight fluctuations over time but the values were under 10 μA for most of the monitored periods, and I_{corr} ranged from 0.6 to 47.5 μA . In case of SL-5 sample, corrosion current values showed a plateau trend from 190 to 390 days, showed slight fluctuations with time but the values were under 10 μA for most of the periods, and I_{corr} ranged from 0.5 to 36.2 μA .

Figure 4 displays the evolution of corrosion current (I_{corr}) with time for FA single rebar samples under various size solution reservoirs as determined by the LPR method. For 17.5 cm solution reservoir length, it is found that all the samples (FA-7, FA-8, and FA-9) showed oscillating trend in terms of corrosion current with time. Samples FA-8 and FA-9 were terminated at around day 620. I_{corr} values ranged from 4.8 to 69.8 μA for FA-7 sample, 5.1–90.0 μA for FA-8 sample, and 7.0–42.8 μA for FA-9 sample. It is to be mentioned that FA-8 and FA-9 samples were terminated after approximately 600 days. It is noticed when examining the I_{corr} plots for 7.5 cm solution reservoir length that the FA-4, FA-5, and FA-6 samples also displayed an oscillating pattern over time. I_{corr} values for FA-4 sample, FA-5 sample, and FA-6 sample varied from 7.6 to 45.5 μA , 8.6–45.4 μA , and 8.3–81.8 μA , respectively. While observing the 5 cm solution reservoir length, it is interesting to note that FA-1 and FA-2 samples showed certain fluctuations in terms

Table 4 Average: Rs, Rc, and Icorr obtained from LPR/EIS readings – SL specimens

Sample Number	Reservoir Length (cm)	Average values from LPR/EIS		
		Rs (kΩ)	Rc (kΩ)	Icorr (μA)
SL-1*		-	-	-
SL-2*	17.5	-	-	-
SL-3		1.8	0.9	33.1
SL-4	2.5	16.9	8.6	6.0
SL-5		14.6	4.2	6.5
SL-6		6.2	2.1	13.7
SL-7	5	5.6	2.9	11.9
SL-8		5.6	3.5	10.2
SL-9		2.0	1.1	25.8
SL-10	10	2.3	1.7	16.4
SL-11		1.9	1.2	22.9

Note: (*) stands for those specimens that had been terminated

Table 5 Average: Rs, Rc, and Icorr obtained from LPR/EIS readings – FA specimens

Sample Number	Reservoir Length (cm)	Average values from LPR/EIS		
		Rs (kΩ)	Rc (kΩ)	Icorr (μA)
FA-1		5.4	3.2	10.4
FA-2	5	6.3	3.6	9.9
FA-3		5.2	2.3	13.2
FA-4		3.0	1.8	16.4
FA-5	7.5	2.3	1.3	21.5
FA-6		3.3	1.7	18.4
FA-7		1.8	1.4	22.6
FA-8*	17.5	-	-	-
FA-9*		-	-	-
FA-10	2.5	11.8	7.7	3.8
FA-11		16.5	7.7	3.5

Note: (*) stands for those specimens that had been terminated

of Icorr over time, and the values were less than 20 μA throughout most of the monitored period. Icorr values ranged from 3.1 to 20.0 μA and 2.0–65.9 μA for FA-1 and FA-2 samples, respectively. The rebar embedded in FA-3 sample showed an oscillating Icorr trend over time and corrosion current values ranged from 6.0 to 45.7 μA. In case of 2.5 cm solution reservoir length, it is observed that FA-10 sample showed a decreasing trend initially, reached a peak value at day 480, and Icorr values ranged from 2.2 to 31.6 μA. FA-11 sample showed a significant decrease initially, therefore followed slight fluctuations with time, and Icorr ranged from 1.3 to 73.5 μA.

Tables 4 and 5 shows average Rs, average Rc, and average Icorr values obtained from the measurements performed from day 750 to day 1100 (last 7 sets of measurements reported in here) using LPR/EIS method. The goal was to acquire a comprehensive assessment of the

corrosion occurring in the rebar embedded within the concrete specimens during this period of time.

Table 4 indicates that the rebars embedded in specimens with the smaller solution reservoir of 2.5 cm had the highest Rs(average) and highest Rc(average) values during the indicated period. However, for the rebars embedded in specimens with the longer solution reservoir of 17.5 cm, the lowest Rs(average) and lowest Rc(average) values were obtained. It was interesting to note that the rebar with the largest average Icorr was the rebar embedded in sample SL-3 with an average value of 33.1 μA, which had the longer solution reservoir of 17.5 cm. The rebar with the lowest average Icorr was for the rebar embedded in SL-4 sample, that had the smaller solution reservoir of 2.5 cm. Icorr average value for SL-4 sample was found to be 6.0 μA.

From Table 5, it was found that the rebars embedded in specimens with the smaller solution reservoir of 2.5 cm had the highest Rs(average) and highest Rc(average) values during the indicated period. On the other hand, the rebars embedded in specimens with the solution reservoir of 17.5 cm had the lowest Rs(average) and lowest Rc(average) values. It was noted that the rebar with the largest average Icorr was the one embedded in sample FA-7, which had a 17.5 cm solution reservoir and an average value of 22.6 μA. The rebar embedded in the FA-11 sample, which had a smaller solution reservoir of 2.5 cm, had the lowest average Icorr value. The FA-11 sample's Icorr average value was found to be 3.5 μA.

During Otieno et al.'s laboratory experiment, they observed significant disparities in the corrosion characteristics between SL (50% GGBS) and FA (30% fly ash) concrete specimens [3]. The study examined concrete specimens with a w/cm ratio of 0.40 and two different cover depths, 40 mm, and 20 mm. The specimens were subjected to an accelerated laboratory corrosion (i.e., cyclic 3 days wetting with 5% NaCl solution followed by 4 days air-drying). These experiments were conducted in a controlled laboratory environment with a temperature of 25±2 °C and a RH of 50±5%. In Otieno's study, an anodic impressed current (IC) was applied to induce an active corrosion state in the specimens. It was assumed that the entire exposed steel surface area of 86 cm² (approximately 27.5 cm long circumferential steel surface) was undergoing corrosion. The SL concrete specimens with a 40 mm cover depth had an average Icorr value of 32.7 μA, while their counterparts with a 20 mm cover depth showed an average Icorr of 44.7 μA [3]. The FA concrete specimens with a 40 mm cover depth exhibited a significantly higher average Icorr value of 91.2 μA, whereas those with a 20 mm cover depth had an average Icorr of 49.9 μA [3]. The age of the specimens at the time of data collection was approximately 854 days, equivalent to 122

weeks. Otieno's findings indicated that all the examined specimens were in a state of high active corrosion.

Hope and Ip conducted experiments on SL samples composed of 50% slag and 50% PC, featuring a w/cm ratio of 0.45 and a cover depth of 56 mm [22]. These specimens underwent multiple wetting and drying cycles, involving immersion in a 3.5% NaCl solution followed by exposure to laboratory air to allow chloride penetration into the concrete. It was assumed that the entire exposed steel surface area of 102 cm² was corroding. Initially, the average I_{corr} values for these concrete specimens were approximately 51 μA during the first 200 days of exposure [22]. Subsequently, as the specimens went through the process of oven-drying, followed by wetting and drying cycles, the average I_{corr} values displayed an upward trend, reaching around 61.2 μA within the exposure period of 270 to 315 days [22]. The results of Hope and Ip's experiment indicated that all the specimens were experiencing a state of high active corrosion.

O'Reilly et al. conducted laboratory experiments involving various types of concrete specimens, including Slag (20) and Slag (40) with 20% and 40% by volume of Grade 100 slag cement, as well as FA (20) and FA (40) with 20% and 40% by volume of Class C fly ash [24]. These specimens all had a w/cm ratio of 0.45 and a cover depth of 25 mm. In O'Reilly's study, the specimens were subjected to alternating exposure cycles, comprising 12 weeks of wet-dry cycles followed by 12 weeks of continuous wet cycles. During the wet-dry cycles, the specimens were ponded with 300 mL of a 15% NaCl solution and maintained at room temperature for 4 days. After this period, corrosion measurements were taken, the salt solution was removed, and the specimens were placed under a heat tent at 100±3 °F (38±2 °C) for 3 days. This cycle was repeated for a total of 12 weeks. Subsequently, the specimens entered a continuously wet cycle, during which they were continuously ponded with a 15% NaCl solution and kept covered at room temperature for another 12 weeks. In O'Reilly's experiment, it was assumed that an exposed steel surface area of 152 cm² was undergoing corrosion. For the Slag samples, the average I_{corr} values were 21 μA for SL (20) and 13.8 μA for SL (40) specimens [24]. Conversely, for the FA specimens, the average I_{corr} values were 38.5 μA for FA (20) and 17.6 μA for FA (40) specimens, respectively [24]. The age of these specimens at the time of data collection was approximately 672 days (96 weeks), during which it was observed that most of the specimens were in a state of high active corrosion. It is important to mention that in the investigations carried out by Otieno et al., Hope and Ip, as well as O'Reilly et al., the corrosion current density values reported were converted into I_{corr} values [3, 22, 24].

It is important to note that any rebar section outside of the concrete as well as any section of the rebar not exactly below the reservoir influenced the corrosion current and other readings. In some instances, the moisture level was so high that the rebar that was exposed to the atmosphere outside the concrete corroded. A corroding site (embedded or not) could act as cathodic protection (prevention) on the rest of the rebar surface, even if chlorides at the rebar surface were high. Current reduction could be indicative that corroding site was not as active or that some area might have re-passivated as suggested by the mix potential measured at later times. A summary of the variation of average corrosion current with length of solution reservoir and concrete mixes are shown graphically in Fig. 5. The average corrosion current values were calculated from the measurements taken from day 750 to day 1100 using LPR/EIS method (last 7 sets of readings). An intriguing observation revealed that, with the increase in the length of the solution reservoir, the corrosion current values also showed a corresponding increase for rebars embedded in both SL and FA concrete mixes. This might be attributed to the increasing length of the solution reservoir, which would result in greater exposure of the rebar surface to chlorides. Consequently, the likelihood of rebar corrosion occurrence could also increase. Furthermore, it is worth noting that, when comparing similar reservoir lengths, the corrosion current values for rebars embedded in SL concrete mixes were larger in comparison to those of rebars embedded in FA concrete mixes.

Theoretical (Faradaic) calculation of mass loss

As no samples in this investigation had any apparent cracks, a theoretical mass loss method was taken into consideration. R_c values were obtained periodically using the LPR and EIS techniques. Corrosion current was generated using the R_c values obtained using the LPR/EIS techniques. Two successive R_c measurements were used to compute the average corrosion current (the average of the two consecutive values for that period). The total amount of charge was then computed by multiplying it by the time difference between each measurement, and each rebar's estimated charge values were added as given in Eq. (1). The apparent mass loss was calculated using Faraday's equation as illustrated in Eq. (2).

$$C = \sum_{N=1}^n \left(\frac{I_N + I_{N-1}}{2} \right) t_N \quad (1)$$

Where C is in coulombs and t is in seconds.

Calculated mass loss by using Faraday's law is given by-

$$\text{Mass Loss} = C * \text{Atomic Mass} / nF \quad (2)$$

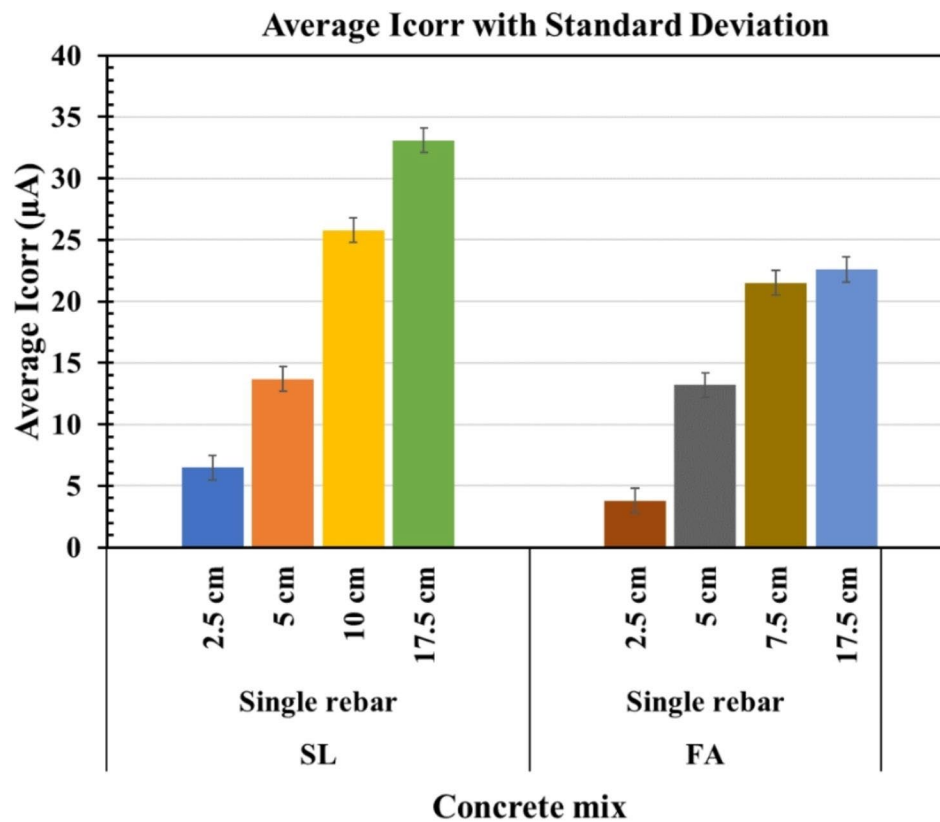


Fig. 5 Variation of average corrosion current with length of solution reservoir and concrete mixes cast with single rebar

Table 6 Estimated Mass loss in grams obtained from LPR readings for SL single rebar samples

Sample Number	Reservoir Length (cm)	Mass Loss (grams)
SL-1*		0.719
SL-2*	17.5	0.690
SL-3		1.186
SL-4	2.5	0.181
SL-5		0.150
SL-6		0.326
SL-7	5	0.528
SL-8		0.344
SL-9		0.740
SL-10	10	0.739
SL-11		0.918

Note: (*) stands for those specimens that had been terminated

Table 7 Estimated Mass loss in grams obtained from LPR readings for FA single rebar samples

Sample Number	Reservoir Length (cm)	Mass Loss (grams)
FA-1		0.254
FA-2	5	0.278
FA-3		0.582
FA-4		0.676
FA-5	7.5	0.603
FA-6		1.002
FA-7		0.565
FA-8*	17.5	0.312
FA-9*		0.306
FA-10	2.5	0.183
FA-11		0.221

Note: (*) stands for those specimens that had been terminated

where Atomic Mass is 55.85 g (for Fe), n is 2 (# of electrons), and F is 96,500 C (Faraday’s constant).

The estimated mass loss in grams for SL and FA single rebar samples obtained using the LPR technique is highlighted in Tables 6 and 7. The presented values are grouped based on the length of the installed solution reservoir. The measurements performed during the monitored period, which lasted around 1100 days, were

used to determine the mass loss values. It is noted that SL-1, SL-2, FA-8, and FA-9 samples (17.5 cm reservoir lengths) were terminated at around 620 days of exposure. The computed mass loss for rebars in SL samples with a 17.5 cm solution reservoir size varied from 0.69 to 1.19 g, while it varied from 0.31 to 0.57 g for rebars in FA samples. Rebars in SL samples exhibited a mass loss ranging between 0.74 and 0.92 g for rebars under 10 cm solution

reservoir size, while it ranged between 0.60 and 1.01 g for FA samples with a reservoir length of 7.5 cm. It was observed that the mass loss values were quite similar and comparable for samples with reservoir lengths of 2.5 cm when comparing the mass loss for SL and FA single rebar samples. For SL samples, longer reservoir length samples (17.5 cm and 10 cm) showed larger mass loss values. For FA samples, it was found that samples with reservoir length of 7.5 cm showed larger mass loss value.

A summary of the variation of average mass loss values with length of solution reservoir and concrete mixes cast with single rebar are shown in Fig. 6. The average mass loss values for different concrete mixes (per reservoir size) were calculated via LPR method from the readings taken throughout the monitored period of approximately 1100 days. An intriguing observation is that as the length of the solution reservoir increases, the average mass loss value also increases for rebars embedded in both SL and FA concrete mixes. However, there was an exception to this trend for FA samples with 7.5 cm reservoir lengths, where the average mass loss value was the largest. As indicated above, four samples (SL-1, SL-2, FA-8, and FA-9) with a reservoir length of 17.5 cm were terminated for forensic examination. The mass loss values were averaged for all the specimens of a specific mix per reservoir size throughout the monitored period, but since four

samples with the larger reservoir length were terminated at day 620, the calculated average values were smaller in comparison to the actual mass loss values (if the samples had not been terminated). It is possible that with time corroding areas under FA samples with 7.5 cm long reservoirs reached or exceeded that observed on FA samples with 17.5 cm long reservoirs.

Concrete beam specimens and corroding cylindrical specimens reinforced with carbon steel rebar of different length were the subjects of experimental research by Torres-Acosta [25]. During preparation, chlorides were added to the concrete mix of these specimens. All specimens were exposed to a RH of 75%. During Torres-Acosta's study, an impressed current of 100 $\mu\text{A}/\text{cm}^2$ was utilized to induce corrosion. In the case of concrete beam samples, the observed mass loss values ranged from 0.3 to 14.4 g based on forensic analysis, and from 0.3 to 12.5 g through Faradaic calculations. For concrete cylindrical specimens undergoing corrosion, the mass loss values ranged from 0.7 to 5.1 g as determined by gravimetric analysis, and from 0.6 to 5.8 g using Faradaic calculation. In Torres-Acosta study, the smaller mass loss corresponded to samples with shorter anode. It was reported that the calculated mass loss values (amount of corrosion products) caused cracks in all the specimens [25], but no cracks were observed by visual inspection in case of

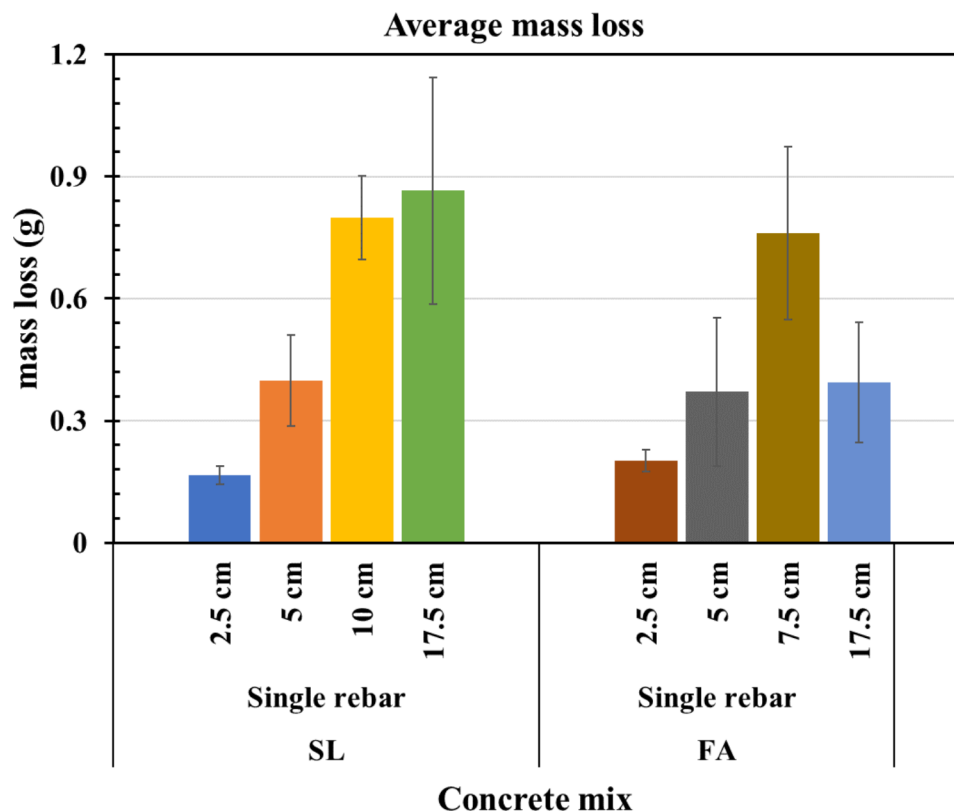


Fig. 6 Variation of average mass loss with length of solution reservoir and concrete mixes cast with single rebar

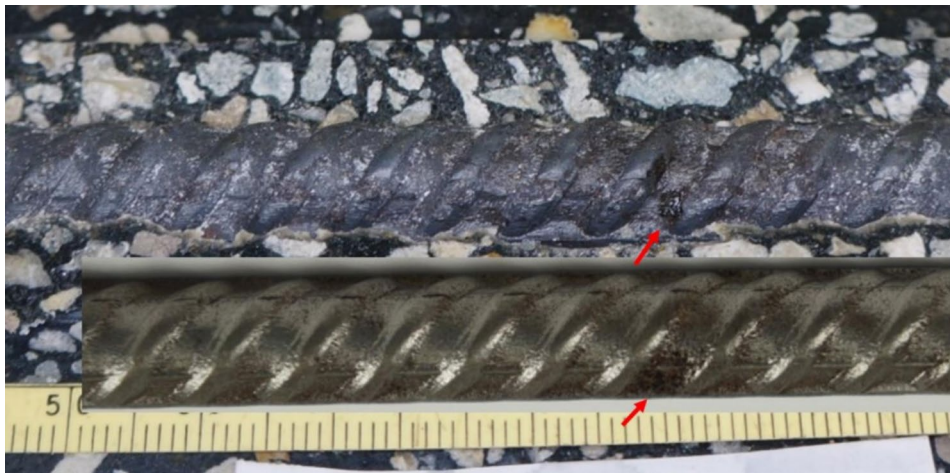


Fig. 7 Before and after cleaning rebar in specimen SL-1 [18, 23]



Fig. 8 Before and after cleaning rebar in specimen SL-2 [18, 23]

current investigation, as it will be shown below that the corrosion in the present study did not take place in the whole rebar, whereas in Torres-Acosta it did.

An experimental investigation was performed on reinforced concrete pipe sections having two different types of concrete compositions [26]. One composition contains fly ash (20% cement replacement), and the other composition contains ordinary Portland cement as the cementitious material. During preparation, chlorides were not added to the concrete mix of these specimens. These specimens were exposed to different environmental conditions. In this investigation, an electromigration technique was employed to initiate corrosion [26]. In the case of compositions containing fly ash exposed to high humidity environment (95% RH, and 21°C), the mass loss values ranged from 2.0 to 10.3 g based on forensic examination, and from 1.9 to 11.3 g by Faradaic calculation. In scenarios [26] where compositions containing ordinary Portland cement were subjected to high humidity environments, the observed mass loss values ranged between 0.6 and 3.2 g based on forensic analysis, and between 1.0 and 3.9 g through Faradaic calculation. The quantity of

corrosion products necessary to cause the concrete to crack may vary depending on the size of the corroding sites, and if the corrosion is all around the reinforcement or localized. In Balasubramanian [26] study, there were several small corroding areas under the reservoir, and the corrosion products penetrated the concrete for a few millimeters. It was found that corrosion was localized on most of the specimens upon forensic analysis, and no cracks were observed in [26]. It can be speculated that smaller corroding sites require greater amount of mass loss to cause concrete cover cracking. The high moisture state of the concrete raises the possibility that the corrosion products may disperse over a wider area rather than concentrating the bursting force in one place.

Forensic analysis

Figure 7 shows that only a small corrosion spot is present on the rebar embedded in specimen SL-1. A modest amount of corrosion is observed in the region after cleaning. The length of the corroding spot is about 3 to 4 mm [18, 23]. Figure 8 shows that there were two corrosion spots on the top surface of the rebar embedded



Fig. 9 Before and after cleaning rebar in specimen FA-8 [18, 23]



Fig. 10 Before and after cleaning rebar in specimen FA-9 [18, 23]

in specimen SL-2. The corroding sites were somewhat deeper on the rebar from SL-2 specimen than the rebar embedded in SL-1 specimen. The solution reservoir was about 17.5 cm long; thus, it appears that corrosion initiated and propagated on a small fraction of the surface subjected to electromigration [18, 23].

Figures 9 and 10 show the rebar surface before and after cleaning on rebars embedded in specimens FA-8 and FA-9, respectively [18, 23]. Figure 9 shows a small corroding site before cleaning on the rebar embedded on specimen FA-8; the cross-section loss is visible but not significant. Figure 10 shows that three corrosion spots developed on the rebar embedded in sample FA-9. The smallest spot is a little hard to see on the picture after cleaning due to the angle of the picture (an arrow indicates the location). The larger corroding spots show a modest but significant cross-section loss; the rebar in specimens FA-9 was subjected to modest anodic current to accelerate corrosion for a short period of time. Both rebars had a solution reservoir of about 17.5 cm long, hence just a small fraction of the area corroded. The opposite side of both rebars showed no corrosion.

General discussion

Accelerated steel corrosion in concrete is needed for timely findings to be obtained in laboratory settings. To examine the corrosion propagation phase in RC structures, particularly in the marine environment, the electromigration method was introduced to initiate corrosion of the embedded rebar. An electric field then drove the chlorides in the solution above each rebar via electromigration method into the concrete and towards the embedded rebar. After a short period of time (weeks/months), corrosion of the embedded rebar started. The

rebar potential and R_c values were used to identify the initiation of the corrosion (R_c values were converted to I_{corr} values). Shortly after the electromigration was stopped, further rebar potential drops were observed. The rebar potential values became more negative than -0.200 Vsce for most of the samples, indicating that the accelerated chloride transport method was successful in initiating corrosion (immediately or after a certain period from suspending electromigration) of the rebars embedded in high-performance concrete specimens.

EIS and LPR measurements were effective in monitoring the corrosion potential, R_s , R_c , and I_{corr} values. During the corrosion propagation stage, the values sometimes fluctuated. In some instances, the rebar potential and accompanying R_c value shifted toward more positive potentials and larger R_c values, which are both indicative of lower I_{corr} values. This phenomenon may occur if corrosion progressed more slowly. In other instances, it is hypothesized that the rebar repassivated or that over time, the corroding sites (corroding at slower rates) were polarized to a more positive value by the non-corroding portion of the rebar.

Several types of rebar potential transients were observed throughout the monitored period. The transient might sometimes be influenced by the concrete's composition, the size of the solution reservoir, total ampere-hour applied, and other factors such as the moisture content at rebar depth, oxygen availability, and relative humidity around the samples.

The samples were kept inside in a lab setting with a reasonably high humidity environment. All the samples had a section of the rebar that was exposed outside of the concrete that was originally uncovered. In a few instances, the rebar was found to have droplets of

moisture that formed due to the high humidity environment, which in some cases led to the outer rebar portion corroding. In other cases, the solution that had filled the reservoir spilled outside, reaching the rebar rather than the concrete. This could lead to corrosion in the extended rebar section, which might potentially have an impact on the measured rebar potential values and corrosion rates. After around 500 days of corrosion propagation period, the rebar section extending outside of the concrete was wire-brushed, sanded, and then covered with shrinkage wrap to limit any corrosion of the rebar surface. As compared to earlier readings, electrochemical measurements beyond this stage were found to be more consistent.

It has been reported that in some cases, in which chloride-induced corrosion took place rust-stains or cracks were not visible and upon forensic examination a significant cross-sectional loss was observed at the corroding site [27]. It was described that for a purely chloride-induced (pitting) corrosion, the usually assumed model (i.e., corrosion taking place around the whole rebar) appears not to be suitable to describe the occurring processes for several reasons [27]. First, iron dissolution only takes place locally rather than uniformly around and along the entire rebar. Second, the corrosion products are much more soluble, and precipitation is unlikely, near the corroding spot (due to presence of chlorides which enhance solubility). Finally, initiation of chloride-induced corrosion is often associated with local weaknesses in the steel/concrete interface, viz. higher local porosity, which would—for the case of precipitation, additionally prevent formation of expansive pressure. Angst paper documented cases in which corrosion initiated by chlorides and that there were little signs (or no) of corrosion stains at the surface during inspections. It was found that upon terminating, a significant cross-sectional loss was found. Similar observations could be found upon terminating some of the samples from this research work.

Conclusion

In this investigation, the electromigration approach effectively accelerated the transport of chlorides such that corrosion initiated within a few weeks to a few months.

For various concrete mixes, the length of the solution reservoirs had a significant impact on the corrosion current values determined by electrochemical measurements. It was found that the corrosion current value increases as the length of the solution reservoir does for the most of the rebars embedded in concrete specimens. The corrosion current values (last 7 sets of readings) were larger for the rebars that are embedded in specimens prepared with SL mix, followed by specimens prepared with FA mix. The range of average corrosion current values were 6.0–33.1 μA for SL samples, and 3.5–22.6 μA for FA samples.

It was found that the estimated mass loss values increased with reservoir size. For SL samples, the calculated mass loss values ranged from 0.15 to 1.19 g, while for FA samples, they ranged from 0.18 to 1.01 g. The calculated mass loss was smaller for the samples with smaller solution reservoir.

There were no cracks or corrosion products that reached the surface of the concrete in the sample. As most of the specimens were not terminated for forensic study, the actual magnitude of the corroding locations was unknown. The quantity of corrosion products necessary for the concrete to crack may depend on the size of the corroding sites. It is hypothesized that the high moisture content of the concrete allowed the corrosion products to penetrate the pore structure in liquid form without concentrating the bursting force in one place. It is also possible that not enough mass loss has taken place. Throughout the roughly 1100-day monitored propagation period, no cracks or corrosion bleed outs were observed.

Acknowledgements

The authors are indebted to the Florida Department of Transportation (FDOT) for preparing the samples. The authors acknowledge funding from FDOT and from USDOT via a TriDurLE grant. The author also acknowledges Florida Atlantic University. In addition, the authors appreciate the assistance with laboratory work and measurements given by Graduate and Undergraduate students at Florida Atlantic University - Marine Materials and Corrosion Laboratory. The opinions expressed in this paper are those of the authors and not necessarily those of FAU, the FDOT, and TriDurLE.

Author contributions

KH, NM, FP wrote the main manuscript text. KH prepared most of the figures. The sample initial set-up was done by FP and NM (first 300 days). Monitoring and measurements continued till approx. day 1200, most done by KH. Calculated mass and initial analysis done by KH. All authors reviewed the manuscript.

Funding

This research is funded through grants provided by Florida Atlantic University, as well as the National Center for Transportation Infrastructure Durability & Life-Extension (TriDurLE), and the Florida Department of Transportation.

Data Availability

Some or all data that support the findings of this study are available from the corresponding author upon reasonable request.

Declarations

Competing interests

The authors declare no competing interests.

Ethics approval and consent to participate

Not applicable.

Received: 12 September 2023 / Revised: 17 November 2023 / Accepted: 21 November 2023

Published online: 29 November 2023

References

1. Castel A, Vidal T, Francois R, Arliguie G (2003) Influence of steel-concrete interface quality on reinforcement corrosion induced by chlorides. *Mag Concr Res* 55(2):151–160
2. Francois R, Arliguie G (1998) Influence of service cracking on reinforcement steel corrosion. *J Mater Civ Eng* 10(1):14–20
3. Otieno M, Beushausen H, Alexander M (2016) Chloride-induced corrosion of steel in cracked concrete—part I: experimental studies under accelerated and natural marine environments. *Cem Concr Res* 79:373–385
4. Vidal T, Castel A, Francois R (2007) Corrosion process and structural performance of a 17-year-old reinforced concrete beam stored in chloride environment. *Cem Concr Res* 37(11):1551–1561
5. Zhang R, Castel A, Francois R (2009) Serviceability limit state criteria based on steel-concrete bond loss for corroded reinforced concrete in chloride environment. *Mater Struct* 42(10):1407–1421
6. Austin SA, Lyons R, Ing MJ (2004) Electrochemical behavior of steel-reinforced concrete during accelerated corrosion testing. *Corrosion* 60(2):203–212
7. El Maaddawy TA, Soudki KA (2003) Effectiveness of impressed current technique to simulate corrosion of steel reinforcement in concrete. *ASCE J Mater Civ Eng* 15(1):41–47
8. Polder RB, Peelen HA (2002) Characterization of chloride transport and reinforcement corrosion in concrete under cyclic wetting and drying by electrical resistivity. *Cem Concr Compos* 24:427–435
9. Wu J, Li H, Wang Z, Liu J (2016) Transport model of chloride ions in concrete under loads and drying-wetting cycles. *Constr Build Mater* 112:733–738
10. Ye H, Jin X, Fu C, Jin N, Xu Y, Huang T (2016) Chloride penetration in concrete exposed to cyclic drying-wetting and carbonation. *Constr Build Mater* 112:457–463
11. Jung WY, Yoon YS, Sohn YM (2003) Predicting the remaining service life of land concrete by steel corrosion. *Cem Concr Res* 33(5):663–677
12. Otieno MB, Beushausen HD, Alexander MG (2016) Chloride-induced corrosion of steel in cracked concrete—part II: corrosion rate prediction models. *Cem Concr Res* 79:386–394
13. Malumbela G, Moyo P, Alexander M (2012) A step towards standardizing accelerated corrosion tests on laboratory reinforced concrete specimens. *J S Afr Inst Civ Eng (SAICE)* 54(2):78–85
14. Care S, Raharinaivo A (2007) Influence of impressed current on the initiation of damage in reinforced mortar due to corrosion of embedded steel. *Cem Concr Res* 37(12):1598–1612
15. Badawi M, Soudki K (2005) Control of corrosion-induced damage in reinforced concrete beams using carbon fiber-reinforced polymer laminates. *J Compos Constr* 9(2):195–201
16. Masoudi S, Soudki K, Topper T (2005) Post-repair fatigue performance of FRP-repaired corroded RC beams: experimental and analytical investigation. *J Compos Constr* 9(5):441–449
17. Presuel-Moreno F, Balasubramanian H, Wu Y-Y (2013) Corrosion of reinforced concrete pipes: an accelerated approach. *Corrosion 2013*, paper no. C2013-0002551, Houston, TX: NACE
18. Presuel-Moreno F, Nazim M, Tang F, Hoque K, Bencosme R (2018) Corrosion Propagation of Carbon Steel Rebars in high performance concrete. BDV27-977-08 Final Report for FDOT.
19. Feliu V, Gonzalez JA, Feliu S (2007) Corrosion estimates from transient response to a potential step. *Corros Sci* 49(8):3241–3255
20. Gonzalez JA, Miranda JM, Feliu S (2004) Consideration on the reproducibility of potential and corrosion rate measurements in reinforced concrete. *Corros Sci* 46(10):2467–2485
21. Hoque K (2020) Corrosion propagation of reinforcing steel embedded in binary and ternary concrete. *Ph.D. Dissertation*, Department of Ocean and Mechanical Engineering, Florida Atlantic University (FAU), Boca Raton, Florida, USA
22. Hope BB, Ip AKC (1987) Corrosion of steel in concrete made with slag cement. *ACI Mater J* 84(6):525–531
23. Presuel-Moreno F, Hoque K (2019) Corrosion propagation of carbon steel rebar embedded in concrete. *Corrosion 2019*, Nashville, Tennessee, USA
24. O'Reilly M, Omid F, Darwin D (2019) Effect of supplementary Cementitious materials on chloride threshold and corrosion rate of reinforcement. *ACI Mater J Title No 116–M12:125–133*
25. Torres-Acosta AA (1999) Cracking Induced by Localized Corrosion of Reinforcement in Chloride Contaminated Concrete. *Ph.D. Dissertation*, Department of Civil & Environmental Engineering, University of South Florida
26. Balasubramanian H (2019) Initiation and Propagation of Corrosion in Dry cast Reinforced Concrete Pipes with Environmental Effects. *Ph.D. Dissertation*, Department of Ocean & Mechanical Engineering, Florida Atlantic University
27. Angst UM, Elsener B, Jamali A, Adey B (2012) Concrete cover cracking owing to reinforcement corrosion—theoretical considerations and practical experience. *Mater Corros* 63:1069–1077

Publisher's Note

Springer Nature remains neutral with regard to jurisdictional claims in published maps and institutional affiliations.